Structure and Reactivity of Dinitrogen Pentoxide in Small Water Clusters Studied by Electronic Structure Calculations

Jonathan P. McNamara and Ian H. Hillier*

Department of Chemistry, University of Manchester, Manchester, M13 9PL, United Kingdom

Received: December 6, 1999; In Final Form: March 13, 2000

High level electronic structure calculations have been used to investigate the mechanism of hydrolysis of dinitrogen pentoxide in small neutral water clusters containing one to six solvating water molecules. The calculations clarify some of the current uncertainties in the hydrolysis mechanism. Increasing the size of the solvating water cluster leads to strong polarization and distortion of the N_2O_5 entity producing incipient (but *not* preexisting) NO_2^+, thus enhancing the electrophilicity of the nitrogen atom. The reaction mechanism involves nucleophilic attack of H_2O on strongly ionized N_2O_5 *followed* by proton transfer to a neighboring water and does not involve the $H_2ONO_2^+NO_3^-$ ion pair. The solvating waters actively participate in the hydrolysis mechanism. The hydrolysis products, *molecular* nitric acid ($HONO_2$) and *ionized* ($H_3O^+NO_3^-$) nitric acid are found to be stable in two different types of structures containing five and six water molecules. For the cluster containing six water molecules, which has a structure related to ice, N_2O_5 is hydrolyzed to yield $H_3O^+NO_3^-$ and $HONO_2$ with essentially no barrier. The calculations thus predict that the hydrolysis of N_2O_5 on PSC ice aerosols can proceed spontaneously in small neutral water clusters. Implications for heterogeneous stratospheric chemistry are discussed.

1. Introduction

The annual appearance of the springtime ozone hole over Antarctica has been attributed to the heterogeneous catalysis of reactions occurring on the surfaces of polar stratospheric cloud (PSC) particles.[1−8] Of particular importance are those reactions that lead to the conversion of chlorine containing reservoir species such as $ClONO_2$, into photochemically active forms of chlorine (Reactions 1−3) which destroy ozone via efficient catalytic cycles.[9−12]

$$ClONO_{2(g)} + HCl_{(s)} \rightarrow Cl_{2(g)} + HNO_{3(s)} \quad (1)$$

$$ClONO_{2(g)} + H_2O_{(s)} \rightarrow HOCl_{(g)} + HNO_{3(s)} \quad (2)$$

$$N_2O_{5(g)} + HCl_{(s)} \rightarrow ClNO_{2(g)} + HNO_{3(s)} \quad (3)$$

$$N_2O_{5(g)} + H_2O_{(s)} \rightarrow 2HNO_{3(s)} \quad (4)$$

However, the hydrolysis of dinitrogen pentoxide (N_2O_5) has also been implicated as an important step in the depletion of stratospheric ozone (Reaction 4).[13−17] N_2O_5 acts as a temporary reservoir for stratospheric NO_x species.[13−17] The atmospheric concentration of N_2O_5 reaches a peak during nighttime as a consequence of the short photolytic lifetime of the NO_3 radical involved in its formation (Reaction 5).[15−17]

$$NO_3 + NO_2 \leftrightarrow N_2O_5 \quad (5)$$

The hydrolysis of N_2O_5 constitutes a major loss pathway for atmospheric nitrogen (NO_x) compounds leading to an increase in catalytically active radicals (e.g., Cl and ClO) thus indirectly promoting ozone depletion.[14] Furthermore, hydrolysis leads to denitrification of the stratosphere yielding nitric acid ($HONO_2$) the major end product of nitrogen oxide emissions.[18] $HONO_2$ leads to acidification of rain[13] and through sedimentation is responsible for the formation of type I PSC aerosol—the active sites for further catalytic reactions.[3]

The hydrolysis of N_2O_5 has been the focus of a number of experimental studies. Hanson and Ravishankara have carried out kinetic studies using flow tubes in order to measure reaction probabilities or *sticking coefficients*, γ.[19] Such experiments have shown hydrolysis to be efficient at stratospheric conditions (ca. 180 K) on NAT (Type I PSC),[19,20] water ice (Type II PSC),[19−21] and also sulfate aerosols[22−24] which are found throughout the atmosphere. The reactions of N_2O_5 with large protonated water clusters[25] and also ion-containing clusters[26] to yield nitric acid are also well documented. Experimental findings suggest the hydrolysis reaction is heterogeneously catalyzed since the analogous gas-phase reaction is considered too slow to explain the observed stratospheric chemistry.[18,27−29] However, a reflection−absorption infrared spectroscopy (RAIRS) study by Horn et al.[30] suggests that molecular N_2O_5 is unlikely to play a major role in heterogeneous reactions but will rather react through its decomposition and hydrolysis reaction products, nitric acid, NO_2^+, NO_3^- and H_3O^+. A recent investigation by Koch et al.[31] involving Fourier transform infrared (FTIR) spectroscopy and semiempirical (AM1) calculations suggest the hydrolysis of N_2O_5 is mechanistically similar to that of $ClONO_2$. Semiempirical calculations indicate nitrogen as the most accessible electrophilic site, which is thus susceptible to attack by surface adsorbed species. Nucleophilic attack by the oxygen of a surface water molecule leads to a lengthening of one of the O−N bonds of N_2O_5 although the existence of the ionic intermediate, $H_2ONO_2^+NO_3$, has yet to be confirmed experimentally. The amount of available surface water is believed to determine the lifetime of the $H_2ONO_2^+$ entity and whether the final reaction products are in their *ionized* or *molecular* form.[31]

There are a number of mechanistic issues that have yet to be resolved completely by experiment or theoretical methods, which we address in this work.

10.1021/jp994279l CCC: $19.00
Published on Web 05/16/2000

TABLE 1: Geometric Parameters of N_2O_5

geometric parameter[a]	B3LYP/6-311++G(d,p)	MP2/6-311++G(d,p)	QCISD/6-311G(d)[b]	experiment[c]
$r(N_1-O_2)$	1.188	1.195	1.192	1.188
$r(N_1-O_3)$	1.187	1.197	1.188	1.188
$r(N_1-O_4)$	1.513	1.526	1.470	1.498
$\angle(O_2N_1O_3)$	133.5	133.9	132.9	133.2
$\angle(N_1O_4N_5)$	115.1	111.8	111.8	111.8
$\angle(O_2N_1O_4)$	110.1	110.3		
$\angle(O_3N_1O_4)$	116.4	115.7		
$\theta(O_2N_1O_3O_4)$	175.7	175.8		
$\theta(O_2N_1O_4N_5)$	151.3	148.3	145.0	150.0

[a] Atomic numbering Figure 2a. Distances (Å), angles and dihedrals (deg). N_2O_5 has C_2 symmetry. [b] Grabow et al.[40] [c] Electron diffraction data.[36]

(1) The extent of *polarization* of N_2O_5 along the N−O−N bonds serving to increase the electrophilicity of the nucleophilic nitrogen, particularly the role of water in enhancing this effect.[31]

(2) The existence, or otherwise of the ion $H_2ONO_2^+$.[31]

(3) The role of the PSC ice aerosol in both catalyzing the reaction and whether the product nitric acid is *ionic* or *molecular*.[30,31]

Although there have been many experimental studies[13−34] of the stratospheric chemistry of N_2O_5 there have been only a limited number of theoretical studies and current uncertainties in the hydrolysis reaction remain. Parthiban et al.[35] determined geometries and harmonic frequencies of eight conformers of N_2O_5 at the Hartree−Fock (HF) level and in agreement with experiment[36] the lowest energy structure had C_2 symmetry with its nitro groups rotated ca. 35° out of the central N−O−N plane in a conrotatory manner (Table 1). A number of other ab initio and density functional theory (DFT) investigations have been performed on the C_2 conformer of N_2O_5.[37−40] On the mechanistic side, Hanway and Tao[41] have studied the hydrolysis reaction catalyzed by both one- and two-water molecules at the B3LYP/6-311++G(d,p) level. The reaction products were *molecular* nitric acid and the activation barrier was calculated to be ca. 24 kcal mol^{-1} for the one-water reaction, which was reduced to ca. 20 kcal mol^{-1} when solvated by an additional water molecule. Such barriers are clearly too high to explain the observed ready reaction on ice with an estimated barrier of ca. 6.2 kcal mol^{-1}.[42] A more recent study by Snyder et al.[43] has revealed the gas-phase hydrolysis leading to the *molecular* products, to proceed essentially spontaneously when catalyzed by only four water molecules. However, at stratospheric conditions the observed product involves solvated *ionized* nitric acid ($H_3O^+NO_3^-$).[30,31] Bianco and Hynes[44] have investigated the interaction of N_2O_5 with both three- and four-water clusters at the HF/3-21G level. They suggest the ice-catalyzed reaction may involve the attack of an OH^--like nucleophile on incipient (but *not* preexisting) NO_2^+ and a coupled proton transfer to yield the $H_3O^+NO_3^-$ ion pair. They also suggest the possibility of different N_2O_5 binding sites with differing reactivity. Related atmospheric reactions have been studied, in particular, the direct reactivation of $ClONO_2$ by HCl (Reaction 1)[44−49] and the hydrolysis of $ClONO_2$ (Reaction 2)[49−54] using both ab initio and DFT methods.

In this paper we present the results of DFT calculations designed to understand the reactivity of dinitrogen pentoxide on PSC ice aerosols. The current uncertainties in the hydrolysis mechanism are addressed by cluster models containing between three and six water molecules in which the differing reactivity of N_2O_5 is shown to depend on how the water cluster modifies the structure of N_2O_5. These calculations explore the early suggestions by Bianco and Hynes[44] that a number of different N_2O_5 binding sites may be involved. The reaction mechanism involves nucleophilic attack of H_2O on strongly polarized N_2O_5 *followed* by a proton transfer to an adjacent water. Importantly, N_2O_5 does *not fully* ionize to form the $H_2ONO_2^+NO_3^-$ contact ion pair (CIP) suggested to occur in an aqueous environment.[31] For a cluster containing five water molecules and a six-water cluster structurally *related* to ice, we confirm experimental observations that at stratospherically relevant temperatures the final reaction products contain the *ionized* form of nitric acid, $H_3O^+NO_3^-$. In the six-water cluster *related* to ice, the hydrolysis reaction is found to proceed essentially spontaneously in line with physical chemistry models and previous theoretical work[43] and is consistent with the expected fast reaction on ice.[42] Finally in light of our calculations, the implications for stratospheric chemistry are discussed.

2. Modeling the Ice Surface

The role of the ice surface in low-temperature heterogeneous catalysis has been the focus of a number of experimental and theoretical investigations. However, to date, the construction and orientation of water molecules at the ice surface remains unclear. In contrast the oxygen atoms in bulk hexagonal ice are known to comprise a wurzite lattice, where the protons are distributed throughout the lattice along the O−O bonds according to the Bernal and Fowler ice rules.[55−57]

Experimentally the external surface of an ice film, crystallized on a Pt(111) surface at 90 K has been studied by Materer et al.[58] Using a variety of techniques, LEED, molecular dynamics (MD), and ab initio calculations, they found that the ice surface had full bilayer termination (Figure 1). Combined FTIR spectroscopy and MD/Monte Carlo simulations have been successful in probing the interaction of adsorbates with ice-like surfaces.[59−63] Devlin and Buch have assigned surface water molecules to one of three categories: three coordinated molecules with either dangling hydrogen or dangling oxygen coordination and four coordinated molecules with distorted tetrahedral geometry. These investigations revealed the presence of rings of water molecules on the ice surface large enough to accommodate several adsorbate species and are proposed as the sites for acid ionization.[63]

Theoretically, electronic structure methods have been used to study the interaction of small atmospherically relevant species such as HOCl and HCl with the ice surface. Geiger et al. have used a four-water cluster excised from the ideal surface of hexagonal ice.[64] Similarly Robinson, Brown, and Doren have studied the interaction of HOCl with both $(H_2O)_4$ and $(H_2O)_{26}$ cluster models excised from the ideal hexagonal ice crystal.[65] The mechanisms of atmospheric reactions have also been explored using small water clusters and high level ab initio methods. The mechanism of oxidation of SO_2 by H_2O_2 in water droplets has been elucidated by Vincent et al.[66] and Smith et al. have investigated the process of acid dissociation in water clusters.[67] Calculations of the direct reactivation of $ClONO_2$ by HCl (Reaction 1)[44−49] and the hydrolysis of $ClONO_2$ (Reaction

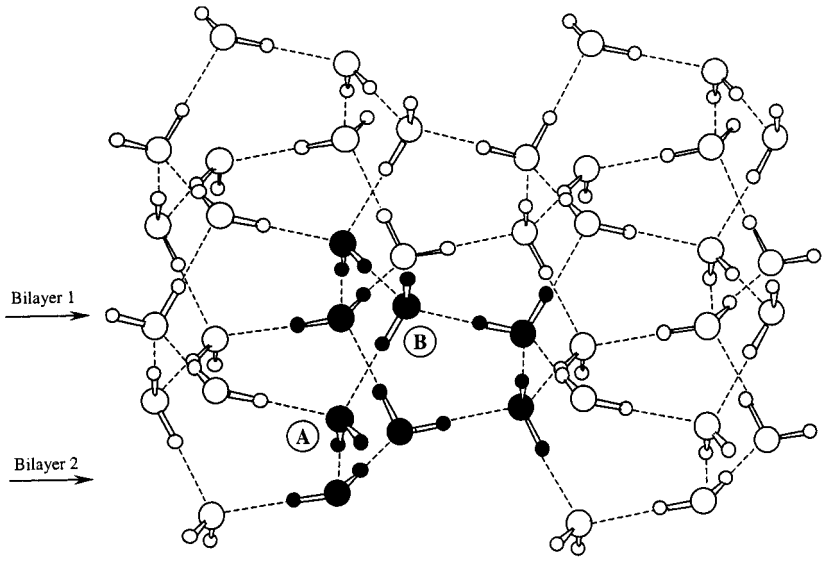

Figure 1. Fragment of proton ordered hexagonal ice, showing water molecules (A, B) removed to accommodate dinitrogen pentoxide.

2)[49−54] in small water clusters have shown these prototypical clusters to reproduce the experimentally observed reactivity of PSC surfaces. Models based on the ideal ice surface may not account for the solvating effect of the ice surface beyond the adsorption site.[64,65] In view of Buch's findings[63] and the proposed dynamic nature of the ice surface[68] we have chosen to study the hydrolysis of dinitrogen pentoxide in water clusters which are relevant to the study of reactions both on the PSC aerosol surface and in small water droplets.

Computational Method

The calculations reported herein have been carried out using the Gaussian 94[69] and Gaussian 98[70] suites of programs. Electron correlation has been included using density functional theory (B3LYP)[71−73] and Møller−Plesset perturbation theory (MP2).[74] For the larger systems studied, DFT was chosen to minimize computational expense, MP2 optimizations being too time-consuming for systems having ca. 380 basis functions. The B3LYP functional was chosen following the recent study by Hanway and Tao,[41] in which the structure of free N_2O_5 calculated at this level is in excellent agreement with the experimental structure (Table 1). Recent electronic structure calculations[45,49,50] have shown that both polarization and diffuse functions are required to describe hydrogen bonded systems. For this reason the flexible 6-311++G(d,p) basis set was used for all DFT optimizations. For comparison single point energy calculations have been carried out at the MP2/6-311++G(3df,-3pd)//B3LYP/6-311++G(d,p) level. Stationary structures were characterized as minima or transition structures (TS) on the potential energy surface by the calculation of harmonic vibrational frequencies. Intrinsic reaction coordinate (IRC) calculations were performed to confirm that *each* TS did indeed connect the reactant and product minima. Due to the size of the systems studied (ca. 380 basis functions) the IRC calculations were restricted to the region close to the TS, the final point in each direction being optimized to obtain the reactant and product complexes. Free energies were calculated within the perfect gas, rigid rotor, harmonic oscillator approximation at 180 K, a temperature appropriate to the stratosphere.

Computational Results

In discussing the various structures we refer to the atomic numbering scheme of the reactant pair (Figure 2a), containing

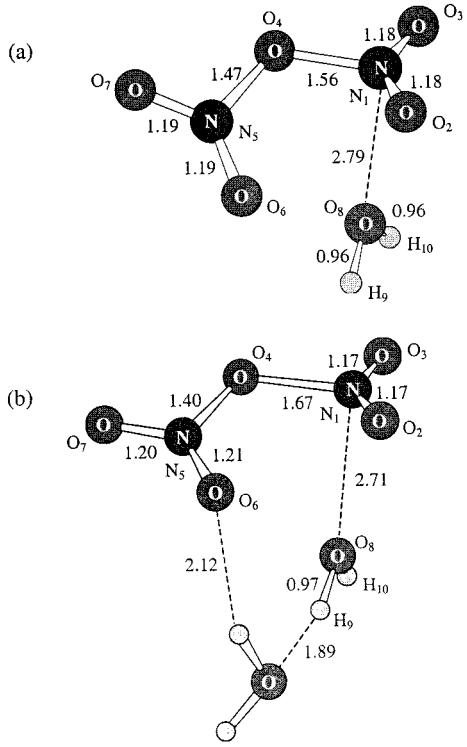

Figure 2. (a) Reactant structure $N_2O_5 \cdot (H_2O)$ showing dinitrogen pentoxide solvated by one water molecule. In this and subsequent Figures, distances are in Å and correspond to the optimized B3LYP/6-311++G(d,p) geometries. (b) Reactant structure $N_2O_5 \cdot (H_2O)_2$ showing dinitrogen pentoxide solvated by two water molecules.

N_2O_5 and the attacking nucleophile, H_2O. The minimum energy structures of dinitrogen pentoxide solvated by one to six water molecules are shown in Figures 2−9. The structures are denoted by the number of *complete* water molecules they contain *before* reaction. Individual structural parameters are at the B3LYP/6-311++G(d,p) level unless otherwise stated. Internal and free energies (180 K) of all structures are given in Tables 2 and 3. When comparing the relative energies of various $N_2O_5 \cdot (H_2O)_n$ isomers, we refer to the difference in free energy (B3LYP) given in Tables 2 and 3. The internal and free energies of binding (Tables 2 and 3) are defined as the difference between the energy of the optimized cluster containing N_2O_5 and the sum of the

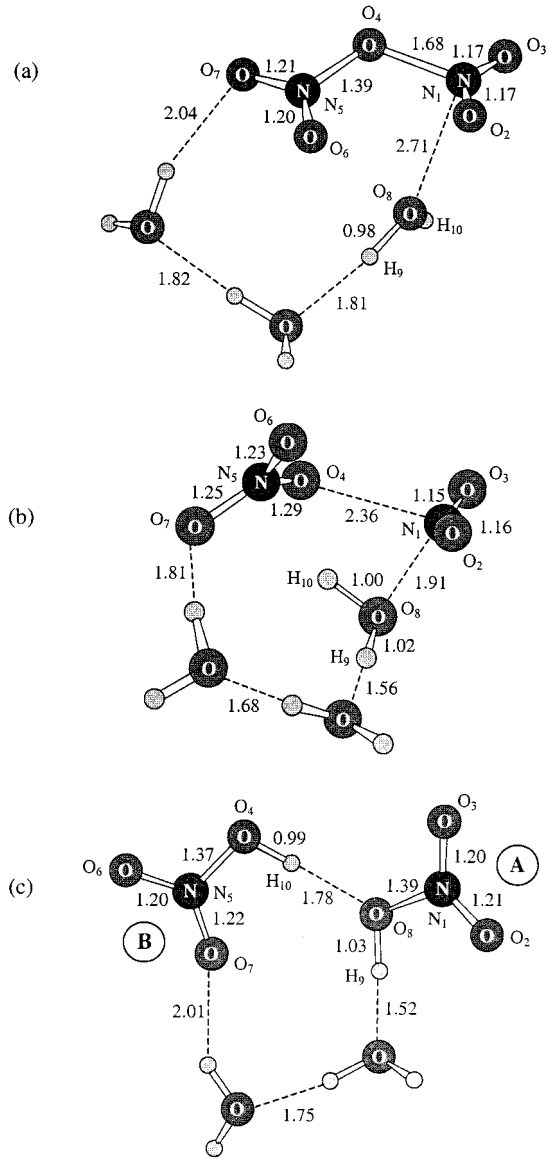

Figure 3. Stationary structures for hydrolysis of $N_2O_5 \cdot (H_2O)_3$ (isomer 2); (a) reactants, (b) transition state, and (c) products ($HONO_2$).

energies for the isolated N_2O_5 and water cluster fragments. The corresponding activation energies are given in Table 4. The minimum energy pathways (MEP) for hydrolysis in 3, 5 (isomer 2), and 6 water clusters derived from the IRC calculations are shown in Figures 10−12 for a thorough analysis of the reaction mechanisms.

A. Gas-Phase N_2O_5. We first consider the gas-phase structure of N_2O_5. Table 1 compares our calculated B3LYP/6-311++G-(d,p) geometry with MP2 and QCISD calculations, and experiment.[36] Our calculated structure is in agreement with a theoretical study by Parthiban et al.[35] who calculated the global minimum structure to have C_2 symmetry with the nitro groups rotated approximately 35° conrotatory out of the central N−O−N plane. The B3LYP structure (Table 1) agrees well with the electron diffraction structure,[36] the largest discrepancy occurring in the calculated $N_1O_4N_5$ angle (115.1°) being a little larger than experiment (111.8°). However the DFT geometry is of comparable quality to the MP2 and QCISD[40] geometries. Having briefly considered the gas-phase structure of N_2O_5 we now consider the structural effects of solvation with one to six water molecules.

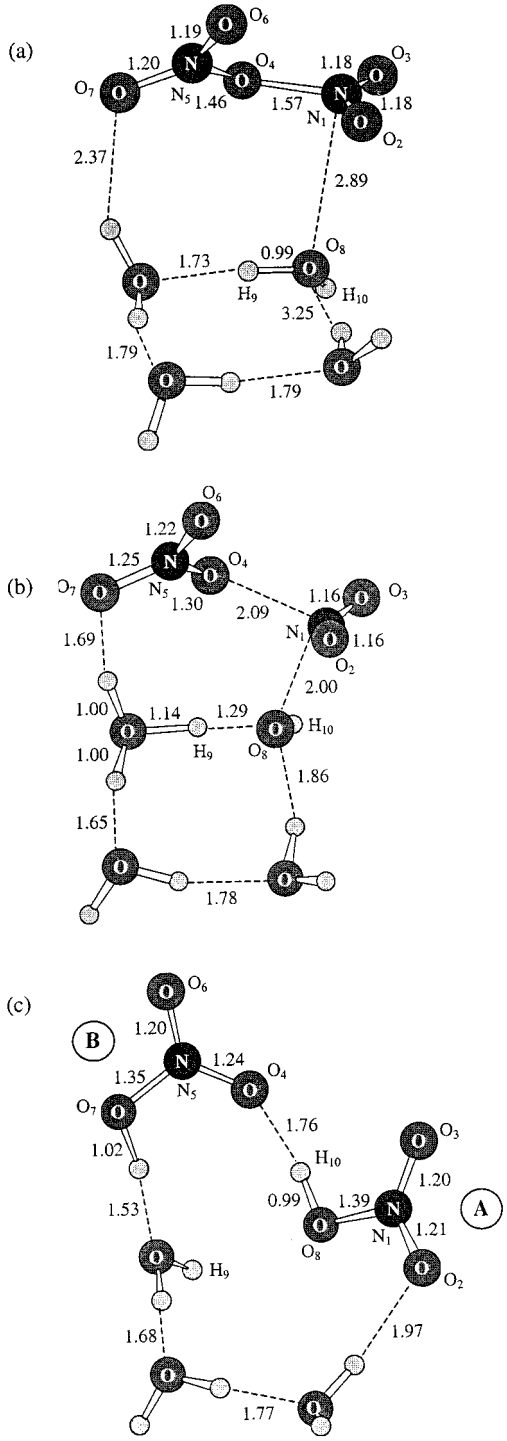

Figure 4. Stationary structures for hydrolysis of $N_2O_5 \cdot (H_2O)_4$; (a) reactants, (b) transition state, and (c) products ($HONO_2$).

Reactivity of N_2O_5. A *reactant structure* is defined as a system in which the breaking N_1-O_4 bond is shorter than the forming N_1-O_8 bond (Figure 2a). Our solvated structures shown in Figures 2−9 illustrate a number of important trends. First, the addition of water molecules leads to a lengthening and shortening of the intra and intermolecular N_1-O_4 and N_1-O_8 distances respectively, consistent with the nucleophilic attack of water at an incipient (but *not* preexisting) $NO_2^{\delta+}$ (atoms N_1, O_2, and O_3) group. A shortening of the O_4-N_5 bond indicates incipient nitrate (atoms O_4, N_5, O_6, and O_7) formation. Mulliken charges (Tables 5 and 6) further support the idea that additional waters enhance ionization leading to a notable polarization of charge within the N_2O_5 entity. The *net* effect is to increase the

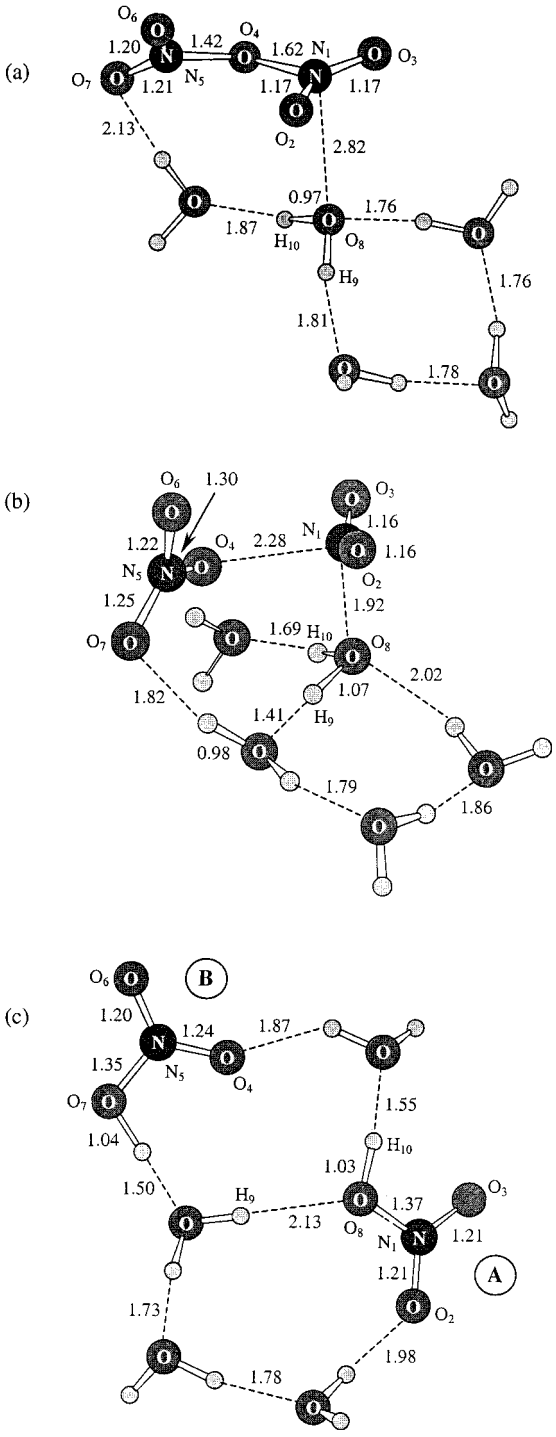

Figure 5. Stationary structures for hydrolysis of $N_2O_5 \cdot (H_2O)_5$ (isomer 1); (a) reactants, (b) transition state, and (c) products ($HONO_2$).

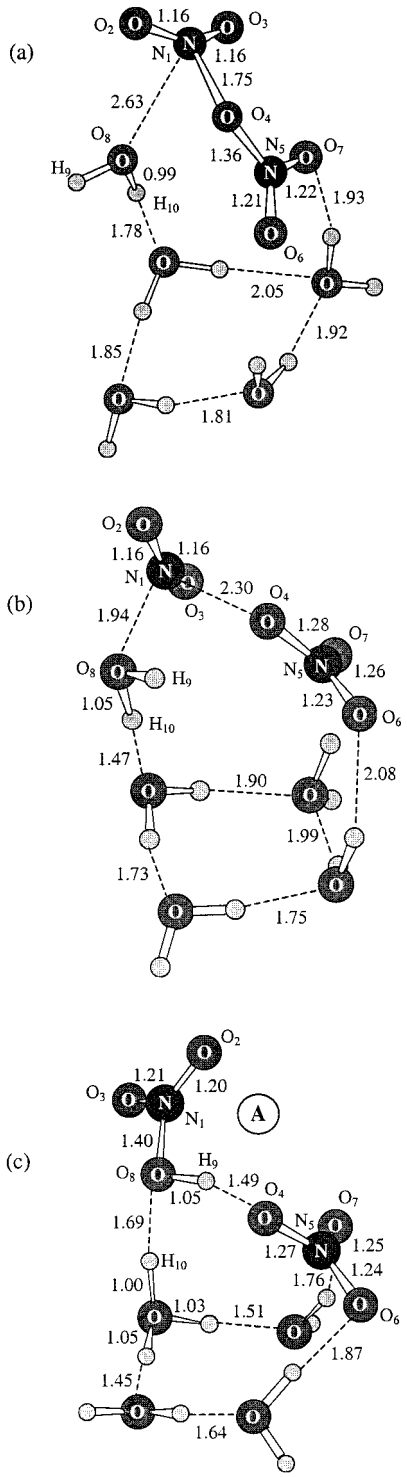

Figure 6. Stationary structures for hydrolysis of $N_2O_5 \cdot (H_2O)_5$ (isomer 2); (a) reactants, (b) transition state, and (c) products ($HONO_2$ and $H_3O^+NO_3^-$).

electrophilicity of the N atom of the $NO_2^{\delta+}$ group. We also note a direct correlation between the increasing ionicity of the N_2O_5 species and the increase in binding energy to the water cluster (Tables 2 and 3). Finally, we note that increasing the number of solvating water molecules reduces the hydrolysis barrier somewhat (Table 4). However, in line with the proposals by Bianco and Hynes[44] and in opposition to the suggestions by Koch et al.[30] the reactant structures indicate N_2O_5 does *not fully* ionize to form the $NO_2^+NO_3^-$ contact ion pair. Thus the calculations argue against the formation of the $H_2ONO_2^+NO_3^-$ CIP in an aqueous environment. The important structural parameters, charge distributions and energetics of our cluster models are now discussed.

B. Ring Structures. We have considered a range of clusters in which N_2O_5 is solvated by one to six water molecules, where the arrangement of the water molecules is related to the rings of waters reported on the ice surface by Buch et al.[63] These rings are suggested to be large enough to accommodate several adsorbate species and are also proposed as the sites for acid ionization in heterogeneous reactions. As a consequence of the proposed dynamic nature of the ice surface[68] it is likely that adsorbate molecules will be further solvated by surface bound waters. Thus we now consider the structure and reactivity of

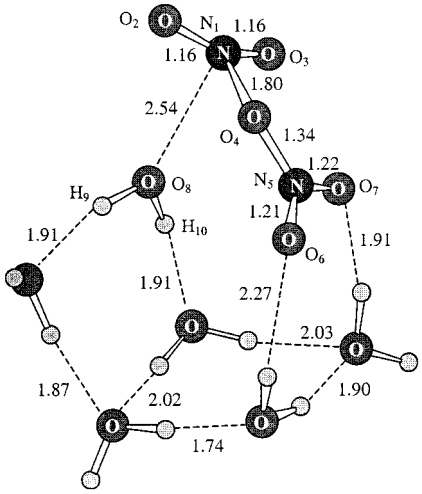

Figure 7. Reactant structure $N_2O_5 \cdot (H_2O)_6$ showing dinitrogen pentoxide solvated by six water molecules.

N_2O_5 solvated in rings of water molecules relevant to the study of the reaction on the PSC surface.

Our initial model structures contain N_2O_5 solvated by one (Figure 2a) and two (Figure 2b) water molecules and have previously been used to study the gas-phase hydrolysis of dinitrogen pentoxide by Hanway and Tao.[41] In their DFT study, the barriers for hydrolysis leading to *molecular* nitric acid ($HONO_2$), were calculated to be 24.0 kcal mol^{-1} and 19.7 kcal mol^{-1} respectively for the one- and two-water reactions (Table 4). The decrease in barrier on the addition of an extra catalytic water thus suggests catalysis on an ice-like surface may be favored.[41] Furthermore, the reduced binding free energies (Table 2) for the one- (-5.0 kcal mol^{-1}) compared to the two-water cluster (-3.2 kcal mol^{-1}), indicate N_2O_5 will not be bound in these clusters, suggesting homogeneous catalysis to be unfavorable.

Solvation by one water molecule (Figure 2a) leads to a lengthening of the N_1-O_4 bond to 1.56 Å (1.51 Å free molecule) and a shortening of the O_4-N_5 bond compared to the free molecule case (Table 1). There is also a weak intermolecular bond between the oxygen of the attacking water and N_1 (2.79 Å). By comparison with the gas-phase geometry of N_2O_5 (Table 1), solvation with two water molecules (Figure 2b) promotes further ionization of N_2O_5 (N_1-O_4, 1.67 Å and O_4-N_5, 1.40 Å). Analysis of the Mulliken charges (Table 5) for the N_2O_5 entity in the two-water cluster indicates a notable polarization of this molecule being 0.18 and -0.12 on the $NO_2^{\delta+}$ and $NO_3^{\delta-}$ groups, respectively. We note that the lengthening and thus weakening of the N_1-O_4 bond allows some rotation of the nitro groups. In view of the large barrier for hydrolysis by two water molecules we now consider the reaction catalyzed by three water molecules.

An additional ring-water molecule has been added to the two-water ring cluster (Figure 2b) to form a three-water cluster (Figure 3a). We note that the arrangement of the water molecules within the three-water cluster could also be related to a fragment excised from the surface of a hexagonal ice lattice.[49−51] In a related three-water system studied by Snyder et al.,[43] the extra solvating water is on the opposite side of the N_2O_5 species and thus two oxygens of the forming nitrate are solvated. The free energy barrier (Table 4) for hydrolysis is calculated to be 13.3 kcal mol^{-1} (14.7 kcal mol^{-1}, MP2), a decrease of 6.4 kcal mol^{-1} from the two-water catalyzed pathway,[41] clearly showing the catalytic effect of the extra solvating water molecule. The energy barrier is a little higher than that calculated for the three-water

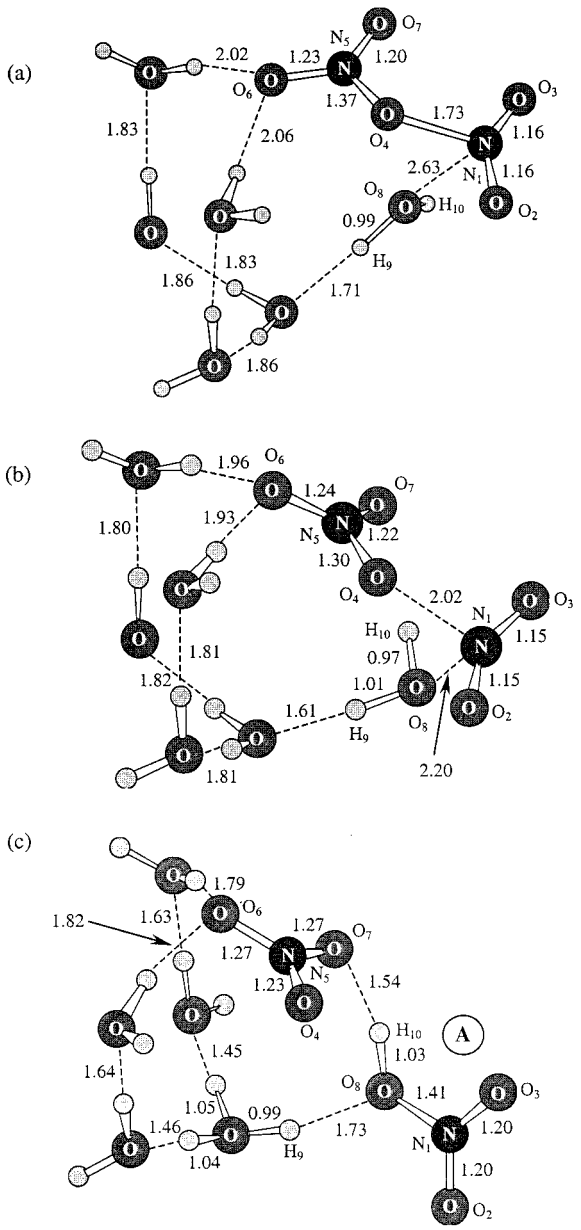

Figure 8. Stationary structures for hydrolysis of $N_2O_5 \cdot (H_2O)_6$; (a) reactants, (b) transition state, and (c) products ($HONO_2$ and $H_3O^+NO_3^-$).

system studied by Snyder et al.[43] (13.0 kcal mol^{-1}). Again, increasing the number of solvating water molecules causes a lengthening of the N_1-O_4 bond (from the isolated molecule, Table 1), to 1.68 Å in this case, a value that is essentially the same as that in the two-water structure. The MEP (Figure 10) involves the attack of O_8 at the electrophilic site N_1 leading to an increase in the N_1-O_4 distance to 2.36 Å in the TS. Associated with these structural changes is a charge transfer from the attacking water to the N_2O_5 entity, with net charges of -0.71 (NO_3), 0.23 (NO_2), and 0.46 (H_2O) indicating ionization is well advanced. The path to the products (*molecular* nitric acid) is characterized by complete cleavage of the N_1-O_4 bond and proton transfer (H_{10}) to O_4 of the departing nitrate group. The hydrolysis mechanism within our three-water cluster differs from that found by Snyder et al.,[43] where a proton of the attacking water is transferred to an adjacent water molecule, whereas for the pathway we have identified the proton is transferred directly onto O_4 of the nitrate entity.

To study the effect of increasing the number of water molecules in the cluster, we have added two additional solvating

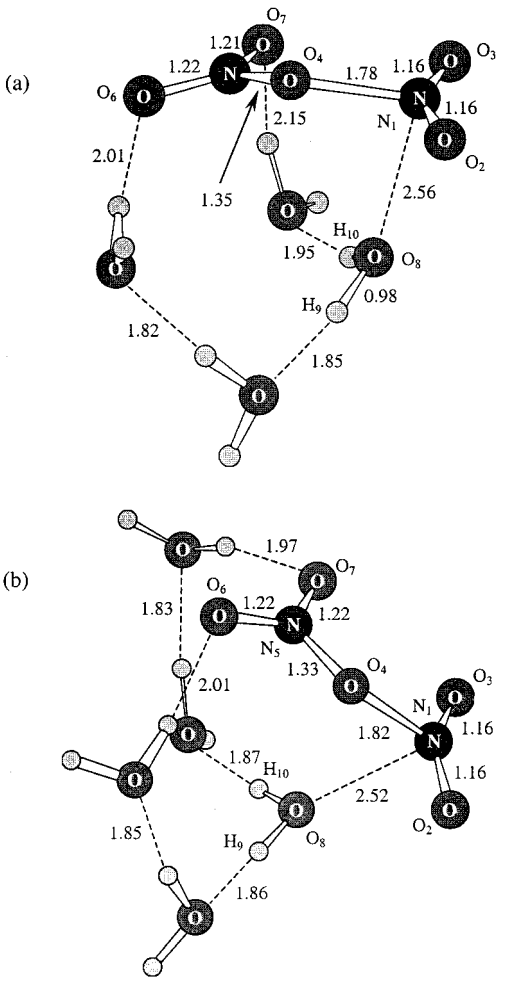

Figure 9. (a) Reactant structure $N_2O_5 \cdot (H_2O)_4$ showing dinitrogen pentoxide solvated by four water molecules. (b) Reactant structure $N_2O_5 \cdot (H_2O)_5$ showing dinitrogen pentoxide solvated by five water molecules.

waters to the two-water cluster (Figure 2b) forming a tetramer-ring, where the extra waters are not directly solvating N_2O_5 (Figure 4a). Structurally the N_2O_5 entity (Figure 4a) is relatively unperturbed from the free molecule case (Table 1) and this is reflected in the binding energy of N_2O_5 (-4.6 kcal mol^{-1}) decreasing by 0.6 kcal mol^{-1} compared to the three-water system (Figure 3a). Importantly, the four-water reactant structure is a stable minimum, differing from the study by Snyder et al.[43] in which no reactant complex could be identified. As far as overall energetics are concerned (Table 4) the barrier for hydrolysis is 19.6 kcal mol^{-1} (21.1 kcal mol^{-1}, MP2) an increase of 6.3 kcal mol^{-1} from the reaction catalyzed by three waters. This increase is expected when comparing the degree of ionization in the three- (Figure 3a) and four-water (Figure 4a) reactant structures. Evidently in the three-water cluster, the enhanced electrophilicity of N_1 due to ionization leads to a lower barrier. We also note that the reaction energy in the four-water cluster has decreased, by 4.3 kcal mol^{-1} to 14.8 kcal mol^{-1}, compared to the three-water reaction. For our four-water cluster the MEP (not shown) differs from the three-water pathway in that the nucleophilic attack is strongly coupled to a proton transfer (H_{10}) to an adjacent water. Thus the TS (Figure 4b) leading to solvated molecular $HONO_2$ (Figure 4c), has most of the positive charge located on a species akin to H_3O^+ as opposed to a protonated nitric acid entity (Figure 3b). Also, evident from the N_1-O_4 and N_1-O_8 distances (2.09 and 2.00 Å), the four-water TS is earlier than in the three-water catalyzed reaction. Hydrolysis within this four-water cluster involves a concerted proton transfer around a two-water ring and is analogous to the pathway identified by Snyder et al.[43] for a three-water system. However, in all the reactions considered thus far, the products involve only *molecular* nitric acid ($HONO_2$), whereas at stratospherically relevant conditions the products involve the *ionized* acid ($H_3O^+NO_3^-$).[30,31] Therefore we now consider the reaction catalyzed by five water molecules.

We have examined two possible structures containing N_2O_5 solvated by five water molecules. Isomer 1 (Figure 5a) is related to the four-water cluster (Figure 4a) where the additional nonring water is in the plane of the tetramer ring. The second cluster (isomer 2, Figure 6a), is closely related to isomer 1, differing in that the extra nonring water is located above the ring. The degree of ionization within isomer 1 is comparable to that in the three-water cluster (Figure 3a) which is expected due to a similar solvating environment around the N_2O_5 entity. However, the increase in ionicity compared to the four-water cluster is reflected in a small increase in the binding energy of 1.7 kcal mol^{-1} (Table 2). We have located a TS (Figure 5b) corresponding to transfer of the $NO_2^{\delta+}$ group to O_8 followed by a proton transfer around the hydrogen bonded ring, to yield the *molecular* products (Figure 5c). Within this structure, the transfer of the $NO_2^{\delta+}$ entity results in a lengthening of the O_8-H_9 bond of the attacking water molecule to 1.07 Å (from 0.97 Å, reactant complex). Charge transfer (Table 5) from the attacking water to the N_2O_5 entity is highlighted by a large positive charge associated with the H_2O entity of 0.29 (0.03, reactant complex) along with developing charges of -0.67 and 0.27 on the incipient $NO_3^{\delta-}$ and $NO_2^{\delta+}$ groups. The barrier for hydrolysis (Table 4) to the *molecular* products, 15.8 kcal mol^{-1}, is 2.5 kcal mol^{-1} higher than for the three-water catalyzed reaction. However, the barrier has decreased by 3.8 kcal mol^{-1} compared to the analogous four-water cluster (Figure 4a) showing the catalytic effect of the addition of a single water molecule (Table 4). The reaction energy is calculated to be -19.7 kcal mol^{-1} and is the most stable product complex (relative to the reactants) of the systems considered so far.

The second five-water system, isomer 2, is 3.2 kcal mol^{-1} (B3LYP) higher in energy (Table 2) than isomer 1 (1.2 kcal mol^{-1}, MP2). The barrier for hydrolysis within this cluster is 7.7 kcal mol^{-1} and the reaction energy is -17.1 kcal mol^{-1} (Table 4). Evidently catalysis by five water molecules in this cluster has significantly lowered the barrier and is in line with that estimated by Tabazadeh et al.[42] using a physical chemistry model (6.2 kcal mol^{-1}). The reactant structure (isomer 2, Figure 6a) contains an N_2O_5 species that is a little more ionized than in the corresponding isomer 1 structure (Figure 5a). The initial portion of the reaction path (Figure 11) involves the attack of the nucleophile (H_2O) at N_1 leading to a notable distortion of N_2O_5 in the TS (Figure 6b). The O_8-H_{10} bond of the attacking water has lengthened a little to 1.05 Å (0.99 Å, reactant complex) and a charge of -0.70 on the $NO_3^{\delta-}$ group indicates the closeness to products of the TS. Collapse of the TS involves transfer of the $NO_2^{\delta+}$ moiety to the water and proton transfer to an adjacent water, yielding the *ionic* products (Figure 6c), solvated $HONO_2$ and $H_3O^+NO_3^-$. Formal charges of 0.71 (H_3O) and -0.72 (NO_3) are evidence for well-defined hydroxonium and nitrate ions (Table 5). Thus the reaction products are in line with experimental observations at stratospheric conditions where the reaction products contain *ionized* nitric acid.[30,31] In the product structure (Figure 6c) the solvated ion pair ($H_3O^+NO_3^-$) is separated by both a layer of water molecules and the molecular acid ($HONO_2$). On a PSC surface it is likely

TABLE 2: Internal and Free Energies (Hartrees) and Binding Energies (kcal mol^{-1}) of Ring Structures

	internal energy (0 K)			free energy (180 K)		
structure[a]	B3LYP/6-311++G(d,p)	MP2/6-311++G(3df,3pd)[b]	binding of N_2O_5[c]	B3LYP/6-311++G(d,p)	MP2/6-311++G(3df,3pd)[d]	binding of N_2O_5[c]
N_2O_5						
	−485.481433			−485.471764		
$N_2O_5 \cdot (H_2O)$[e]						
	−561.945455	−560.985303	3.98	−561.915739	−560.955587	−5.04
$N_2O_5 \cdot (H_2O)_2$[f]						
	−638.416118	−637.323472	8.52	−638.362636	−637.269990	−3.23
$N_2O_5 \cdot (H_2O)_3$[g]						
(R)	−714.890055	−713.663750	11.06	−714.811550	−713.585245	−3.99
(TS)	−714.871016	−713.642439		−714.790388	−713.561811	
(P)	−714.922408	−713.685091		−714.841976	−713.604659	
$N_2O_5 \cdot (H_2O)_4$[h]						
(R)	−791.370226	−790.007428	4.06	−791.267868	−789.905070	−4.58
(TS)	−791.339499	−789.974305		−791.236607	−789.871413	
(P)	−791.394375	−790.022271		−791.291442	−789.919338	
$N_2O_5 \cdot (H_2O)_5$						
isomer 1[i](R)	−867.840572	−866.343841	6.96	−867.715398	−866.218667	−2.93
(TS)	−867.817183	−866.322437		−867.690225	−866.195479	
(P)	−867.873604	−866.366006		−867.746820	−866.239222	
isomer 2[j](R)	−867.837395	−866.343847	16.18	−867.710255	−866.216707	6.38
(TS)	−867.827744	−866.329914		−867.697933	−866.200103	
(P)	−867.866373	−866.359995		−867.737448	−866.231070	
$N_2O_5 \cdot (H_2O)_6$[k]						
	−944.312670	−942.685998	20.37	−944.160118	−942.533446	10.40

[a] R (Reactants), TS (Transition State) and P (Products). [b] Single point energy evaluations using B3LYP/6-311++G(d,p) structures. [c] B3LYP/6-311++G(d,p) level. [d] Includes thermodynamic correction at B3LYP/6-311++G(d,p) level. [e] Figure 2a. [f] Figure 2b. [g] Figure 3. [h] Figure 4. [i] Figure 5. [j] Figure 6. [k] Figure 7.

TABLE 3: Internal and Free Energies (Hartrees) and Binding Energies (kcal mol^{-1}) of Ice-like Structures

	internal energy (0 K)			free energy (180 K)		
structure[a]	B3LYP/6-311++G(d,p)	MP2/6-311++G(3df,3pd)[b]	binding of N_2O_5[c]	B3LYP/6-311++G(d,p)	MP2/6-311++G(3df,3pd)[d]	binding of N_2O_5[c]
$N_2O_5 \cdot (H_2O)_4$[e]						
	−791.359635	−790.001397	17.03	−791.257878	−789.899640	5.94
$N_2O_5 \cdot (H_2O)_5$[f]						
	−867.832950	−866.340226	21.84	−867.708470	−866.215746	12.08
$N_2O_5 \cdot (H_2O)_6$[g]						
(R)	−944.306138	−942.678236	18.30	−944.158068	−942.530166	7.05
(TS)	−944.303464	−942.671637		−944.152728	−942.520901	
(P)	−944.344282	−942.703119		−944.192027	−942.550864	

[a] R (Reactants), TS (Transition State) and P (Products). [b] Single point energy evaluations using B3LYP/6-311++G(d,p) structures. [c] B3LYP/6-311++G(d,p) level. [d] Includes thermodynamic correction at B3LYP/6-311++G(d,p) level. [e] Figure 9a. [f] Figure 9b. [g] Figure 8.

TABLE 4: Reaction Energies and Barriers (kcal mol^{-1}) and Transition State Imaginary Frequencies (cm^{-1})

		internal energy (0 K)				free energy (180 K)			
	imaginary	B3LYP/6-311++G(d,p)		MP2/6-311++G(3df,3dp)[a]		B3LYP/6-311++G(d,p)		MP2/6-311++G(3df,3dp)[b]	
reaction	frequency	barrier	reaction	barrier	reaction	barrier	reaction	barrier	reaction
ring clusters									
$N_2O_5 \cdot (H_2O)$[c]		24.0	−16.2						
$N_2O_5 \cdot (H_2O)_2$[c,d]		19.7	−28.8						
$N_2O_5 \cdot (H_2O)_3$[e]	−158.6	12.0	−20.3	13.4	−13.4	13.3	−19.1	14.7	−12.2
$N_2O_5 \cdot (H_2O)_4$[f]	−568.1	19.3	−15.2	20.8	−9.3	19.6	−14.8	21.1	−9.0
$N_2O_5 \cdot (H_2O)_5$ (Isomer 1)[g]	−209.3	14.7	−20.7	13.4	−13.9	15.8	−19.7	14.6	−12.9
$N_2O_5 \cdot (H_2O)_5$ (Isomer 2)[h]	−133.4	6.1	−18.2	8.7	−10.1	7.7	−17.1	10.4	−9.0
ice-like clusters									
$N_2O_5 \cdot (H_2O)_6$[i]	−116.1	1.7	−23.9	4.1	−15.6	3.4	−21.3	5.8	−13.0

[a] Single point energy evaluations using B3LYP/6-311++G(d,p) structures. [b] Includes thermodynamic correction at B3LYP/6-311++G(d,p) level. [c] Hanway and Tao.[41] [d] B3LYP/6-311++G(d,p)//6-31G(d). [e] Figure 3. [f] Figure 4. [g] Figure 5. [h] Figure 6. [i] Figure 8.

that the *molecular* acid will be further solvated and ionize following the reaction, since two ion pairs are unlikely to be formed in the initial step. We note that the product structure containing *ionized* nitric acid (Figure 6c) is a little higher in energy (5.9 kcal mol^{-1}) than the product structure containing only *molecular* nitric acid (Figure 5c). Compared to the three-water reaction, the key bonding changes, such as proton transfer, occur at similar points along the MEP (Figures 10 and 11).

Finally, we have investigated the structural effect on N_2O_5 of the addition of a further solvating water added to the five-water cluster (isomer 2, Figure 6a) to form a six-water system (Figure 7). The additional solvating water is located above the tetramer-ring and thus accounts for the solvating effect of surface bound water molecules. In line with the clusters considered so far, the six-water reactant structure (Figure 7) contains significantly ionized N_2O_5. Compared to the five-water cluster (isomer

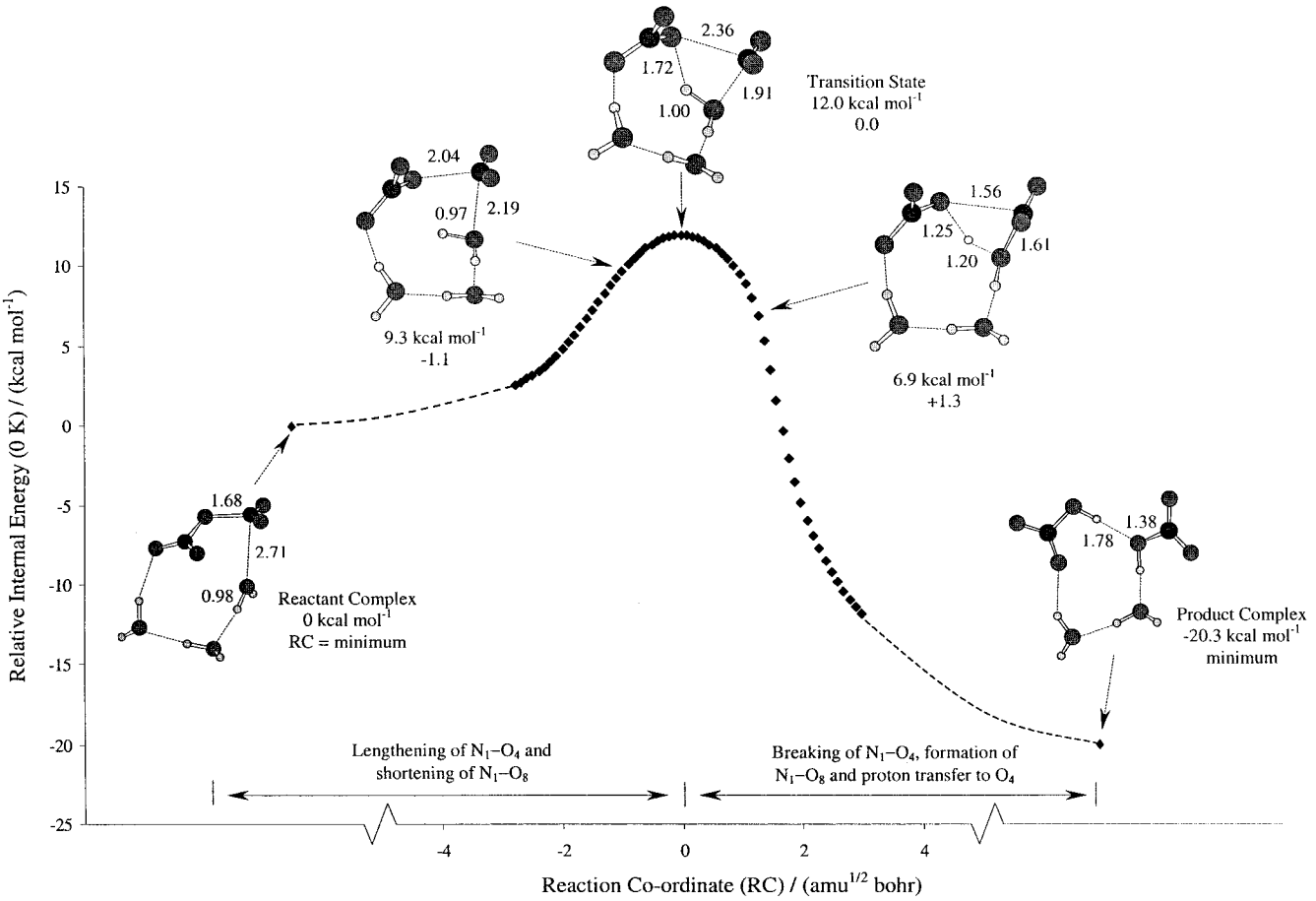

Figure 10. Minimum energy pathway for hydrolysis in $N_2O_5 \cdot (H_2O)_3$ cluster.

2) the binding energy has increased by 4 kcal mol^{-1} to 10.4 kcal mol^{-1}. Clearly the addition of an extra surface-bound solvating water has increased the ionicity of the N_2O_5 entity compared to the five-water cluster (isomer 2, Figure 6a). Given the relatively low barrier leading to the *ionic* products (7.7 kcal mol^{-1}) for hydrolysis in the related five-water cluster no TS search was carried out.

Following our study[49,50] in which $ClONO_2$ was calculated to hydrolyze essentially spontaneously in a six-water cluster *related* to hexagonal ice, we now consider the structure and reactivity of N_2O_5 solvated in ice-like clusters

C. Ice-like Structures. Combined LEED and MD simulations by Materer et al.[58] suggest the surface of ice has complete bilayer termination. We have investigated the reactivity of N_2O_5 in a six-water cluster, generated by replacing the surface bilayer water molecules (A, B Figure 1) of such a proton-ordered phase of hexagonal ice, with a N_2O_5 molecule.

The extent of ionization of the N_2O_5 entity within this six-water reactant structure (Figure 8a) is similar to that in the six-water ring structure (Figure 7) as evident from a small decrease in the binding energy of 3.4 kcal mol^{-1} (Tables 2 and 3). The MEP (Figure 12) displays some differences from those calculated for the three- and four-water reactions. The early part of the reaction involves the attack by H_2O at N_1 leading to a lengthened N_1-O_4 distance of 2.02 Å in the TS (Figure 8b), notably less than in the five-water reaction (2.30 Å, Figures 6 and 11). An increase in the positive charge associated with H_2O (by 0.29) is evidence for charge transfer to the N_2O_5 entity (Table 6). A formal charge of −0.46 is associated with a species akin to NO_3 and shows the closeness to products of the TS. The barrier for hydrolysis of N_2O_5 is 3.4 kcal mol^{-1} (B3LYP) and the reaction energy −21.3 kcal mol^{-1} (Table 4). A similar barrier is predicted at the MP2 level (5.8 kcal mol^{-1}), while at this level the reaction products are calculated to be notably less stable (−13.0 kcal mol^{-1}). Importantly the product structure (Figure 8c) involves *ionized* nitric acid ($H_3O^+NO_3^-$) and *molecular* nitric acid ($HONO_2$). As with the five-water ion pair structure (Figure 6c) the hydroxonium and nitrate ions are separated by the molecular acid and effectively two solvation shells. Clearly the arrangement of the water molecules is suited to stabilizing the hydroxonium ion. Thus hydrolysis in the six-water cluster reproduces the experimentally observed reactivity.[30,31] Having identified a reactive six-water cluster containing solvated N_2O_5 we thus investigated the structural effects on N_2O_5 of solvation in smaller ice-like structures.

We have located minimum energy structures containing N_2O_5 solvated by four (Figure 9a) and five (Figure 9b) water molecules. Both structures are related to the six-water cluster (Figure 8a), but have further waters removed creating larger defects on the full bilayer terminated surface. Removal of the attacking water from the six-water cluster leads to the five-water cluster (Figure 9b). The N_2O_5 entity is ionized to a greater extent than in the five-water ring structures previously considered (Figures 5a and 6a). The increased ionic interaction is evident from a binding energy of 12.1 kcal mol^{-1} (Table 3). The N_1-O_4 bond is notably extended (1.82 Å) whereas the O_4-N_5 bond is compressed to a value of 1.33 Å, indicating incipient nitrate formation. The formal charges (Table 6) further support the concept of charge separation, being 0.34 and −0.30 on the developing $NO_2^{\delta+}$ and $NO_3^{\delta-}$ groups, respectively.

The four-water cluster (Figure 9a) we have identified is similar to the three-water cluster studied by Snyder et al.,[43]

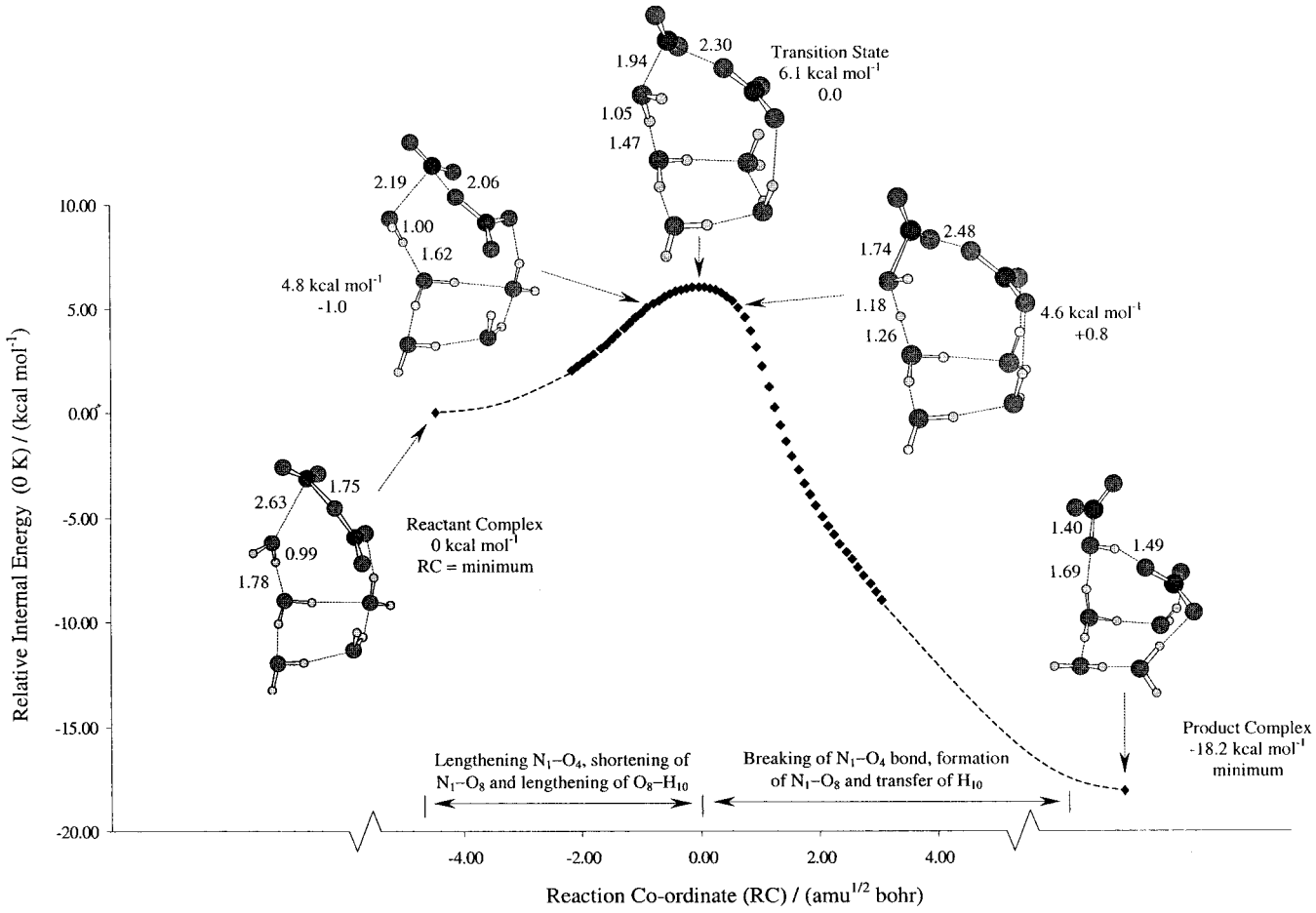

Figure 11. Minimum energy pathway for hydrolysis in $N_2O_5 \cdot (H_2O)_5$ (isomer 2) cluster.

where both O_6 and O_7 of the forming nitrate are solvated. However, they were unable to locate a stable structure containing N_2O_5 solvated by four water molecules. Compared to the four-water ring structure (Figure 4a), N_2O_5 now shows increased ionization evident from an increase in the binding energy by 10.5 kcal mol^{-1}. Furthermore, formal charges (Table 6) of 0.29 ($NO_2^{\delta+}$) and −0.25 ($NO_3^{\delta-}$) indicate that N_2O_5 is considerably more polarized than in the four-water ring structure (Figure 4a). In view of the very low barrier calculated for the reaction in the six-water ice-like cluster, leading to the *ionic* products ($H_3O^+NO_3^-$ and $HONO_2$) no TS searches were carried out for these four- and five-water clusters.

Discussion

We begin by commenting on the method of including electron correlation and the choice of basis set. Our calculations have shown that DFT (B3LYP functional) combined with the 6-311++G(d,p) basis, correctly describes the structure of N_2O_5 itself (Table 1) and is in excellent agreement with both higher level calculations (MP2, QCISD) and electron diffraction data.[36]

The calculations reported herein highlight a number of important details concerning the mechanism of hydrolysis of N_2O_5 on PSC ice aerosols. Our studies confirm that the reactivity of N_2O_5 is controlled by the relative nucleophilic/electrophilic strengths of the species involved. The addition of extra solvating water molecules leads to a notable distortion and polarization of the N_2O_5 reactant species (Figures 2−9). The *net* effect is to increase electrophilicity of N_1 thus making it more susceptible to nucleophilic attack from a surface bound water. Charge separation within the N_2O_5 entity leads to the formation of incipient (but *not* preexisting) $NO_2^{\delta+}$ and $NO_3^{\delta-}$ groups. However in all the binding situations we have considered, N_2O_5 *does not fully* ionize into a stable $NO_2^+NO_3^-$ contact ion pair (CIP) before reaction. These findings are in broad agreement with the mechanism suggested by Bianco and Hynes.[44] However, in opposition to this, Koch et al.[30] believe N_2O_5 ionizes on the ice surface forming $NO_2^+NO_3^-$ which in an aqueous environment would form the $H_2ONO_2^+NO_3^-$ CIP. In the hydrolysis of chlorine nitrate ($ClONO_2$) a protonated acid intermediate (H_2OCl^+) has been shown to exist both theoretically[50] and experimentally.[75−78] The formation of H_2OCl^+ is explained by considering this to be the extreme case of ionization along the O_2NO-Cl bond leading to transfer of the Cl atom to the attacking nucleophile H_2O such that chlorine is closer to the attacking water than the departing nitrate anion. However, Bianco and Hynes[44,51] argue against the formation of both the H_2OCl^+ and $H_2ONO_2^+$ intermediates and our calculations of the N_2O_5 hydrolysis mechanism support the latter. Clearly, in the reactant complexes considered the O−N−O angle in the incipient $NO_2^{\delta+}$ moiety is far from 180° in the calculated $H_2ONO_2^+$ complex at this level (Figure 13). Thus our calculations suggest $H_2ONO_2^+$ is unlikely to be involved in the ice-catalyzed reaction, although further increasing the size of the water cluster may lead to increased ionization of the N_2O_5 entity.

The reaction mechanism (Figures 3, 5, 6, 8, and 10−12) is characterized by an S_N2 attack of H_2O at N_1 of the strongly polarized N_2O_5 which is followed by proton transfer to an adjacent water (or nitrate in the three-water reaction). Importantly the structure of the water cluster (the adsorption site) influences the nature of the bonding changes along the reaction

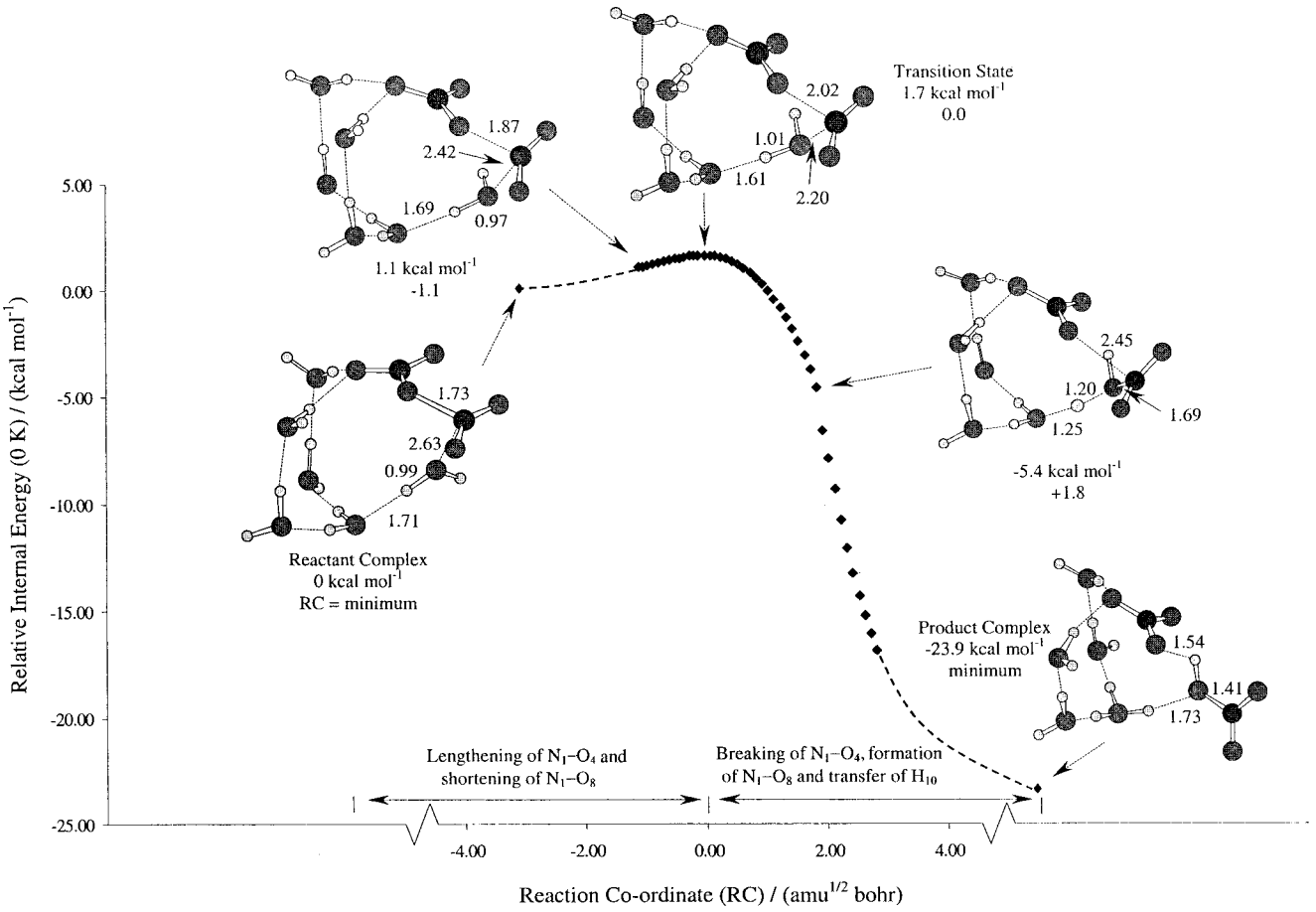

Figure 12. Minimum energy pathway for hydrolysis in $N_2O_5 \cdot (H_2O)_6$ cluster.

TABLE 5: Mulliken Charges (e) of Reactant Pair (Figure 2a) in Ring Clusters

											total charges							
	atomic charges[a]										reactant fragments				product fragments			
structure	N_1	O_2	O_3	O_4	N_5	O_6	O_7	O_8	H_9	H_{10}	N_2O_5	NO_2	NO_3	H_2O	$HONO_2$ (A)	$HONO_2$ (B)	H_3O	NO_3
$H_2ONO_2^+$ [b]	0.44	0.26	0.26					−0.62	0.33	0.33								
N_2O_5	−0.20	0.06	0.06	0.16	−0.20	0.06	0.06				0.00							
$N_2O_5 \cdot (H_2O)$[c]	−0.09	0.07	0.08	0.17	−0.25	0.05	0.03	−0.61	0.29	0.26	0.06	0.06	0.00	−0.06				
$N_2O_5 \cdot (H_2O)_2$[d]	−0.07	0.13	0.12	0.16	−0.31	0.00	0.03	−0.70	0.37	0.28	0.06	0.18	−0.12	−0.05				
$N_2O_5 \cdot (H_2O)_3$[e]																		
(R)	−0.07	0.15	0.11	0.18	−0.38	0.08	0.01	−0.71	0.39	0.26	0.08	0.19	−0.11	−0.06				
(TS)	−0.22	0.23	0.22	−0.14	−0.44	−0.04	−0.09	−0.24	0.43	0.27		0.23	−0.71	0.46				
(P)	−0.26	−0.04	0.00	0.00	−0.37	0.02	−0.05	−0.25	0.52	0.39					−0.03	−0.01		
$N_2O_5 \cdot (H_2O)_4$[f]																		
(R)	−0.36	0.16	0.14	0.22	−0.25	0.05	0.04	−0.64	0.35	0.28	0.00	−0.06	0.06	−0.01				
(TS)	−0.41	0.24	0.23	−0.01	−0.34	−0.05	−0.06	−0.54	0.49	0.25		0.06	−0.46	0.20				
(P)	−0.37	−0.03	0.03	−0.12	−0.33	0.02	−0.04	−0.01	0.26	0.41					0.03	−0.03		
$N_2O_5 \cdot (H_2O)_5$																		
isomer 1[g](R)	−0.36	0.21	0.17	0.21	−0.27	0.02	0.02	−0.71	0.35	0.39	−0.00	0.02	−0.02	0.03				
(TS)	−0.19	0.25	0.21	−0.17	−0.37	−0.05	−0.08	−0.37	0.33	0.33		0.27	−0.67	0.29				
(P)	−0.30	−0.02	−0.02	−0.10	−0.37	0.00	−0.05	−0.14	0.33	0.47					−0.01	−0.03		
isomer 2[h](R)	−0.08	0.14	0.20	0.16	−0.38	0.02	0.01	−0.71	0.25	0.40	0.07	0.26	−0.19	−0.05				
(TS)	−0.20	0.21	0.23	−0.09	−0.48	−0.03	−0.10	−0.30	0.27	0.46		0.24	−0.70	0.43				
(P)	−0.29	0.02	−0.02	−0.10	−0.43	−0.05	−0.14	−0.14	0.37	0.33					−0.06		0.71	−0.72
$N_2O_5 \cdot (H_2O)_6$[i]	−0.09	0.18	0.22	0.15	−0.44	0.01	0.01	−0.72	0.35	0.37	0.04	0.31	−0.27	0.00				

[a] Refer to Figure 2a for atom labeling. R (Reactants), TS (Transition State) and P (Products). [b] Figure 13. [c] Figure 2a. [d] Figure 2b. [e] Figure 3. [f] Figure 4. [g] Figure 5. [h] Figure 6. [i] Figure 7.

pathway. For example, in the four-water catalyzed reaction (Figure 4, MEP not shown) proton transfer occurs such that the TS contains a species akin to H_3O^+ and a relatively short N_1-O_4 bond of 2.09 Å. In contrast in the five-water reaction (Figures 6 and 11) the TS has an N_1-O_4 bond of length 2.35 Å and the O_8-H_{10} bond is only extended a little (1.05 Å). These findings reveal the possibility that a number of different adsorption sites may be present on the ice surface which may

TABLE 6: Mulliken Charges (e) of Reactant Pair (Figure 2a) in Ice-Like Clusters

	atomic charges[a]										total charges							
											reactant fragments				product fragments			
structure	N_1	O_2	O_3	O_4	N_5	O_6	O_7	O_8	H_9	H_{10}	N_2O_5	NO_2	NO_3	H_2O	$HONO_2$ (A)	$HONO_2$ (B)	H_3O	NO_3
$N_2O_5 \cdot (H_2O)_4$[b]																		
	−0.09	0.17	0.21	0.14	−0.44	0.04	0.01	−0.72	0.38	0.36	0.04	0.29	−0.25	0.02				
$N_2O_5 \cdot (H_2O)_5$[c]																		
	−0.08	0.19	0.23	0.14	−0.43	−0.01	0.00	−0.75	0.36	0.41	0.04	0.34	−0.30	0.02				
$N_2O_5 \cdot (H_2O)_6$[d]																		
(R)	−0.14	0.15	0.21	0.17	−0.33	−0.04	0.07	−0.74	0.40	0.26	0.09	0.22	−0.13	−0.08				
(TS)	−0.22	0.24	0.23	0.10	−0.44	−0.07	−0.05	−0.44	0.40	0.25		0.25	−0.46	0.21				
(P)	−0.30	−0.02	0.03	−0.05	−0.47	−0.15	−0.06	−0.10	0.32	0.32					−0.07		0.73	−0.73

[a] Refer to Figure 2a for atom labeling. R (Reactants), TS (Transition State) and P (Products). [b] Figure 9a. [c] Figure 9b. [d] Figure 8.

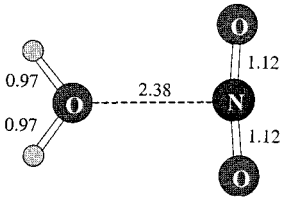

Figure 13. Ion−molecule complex $H_2ONO_2^+$.

also have differing reactivity. The calculations confirm at a molecular level early suggestions regarding the ice-catalyzed hydrolysis of N_2O_5.[44]

Experimentally at stratospheric conditions RAIR spectroscopic studies[30,31] report the reaction products involve only the *ionized* acid ($H_3O^+NO_3^-$). For the reaction catalyzed by three (Figure 3), four (Figure 4) and five (Figure 5) water molecules the reaction products only contain the *molecular* acid ($HONO_2$). Clearly, in each of these reactions, the initial reactant structure contains species close to *molecular* N_2O_5 which is not thought to be involved in heterogeneous catalysis.[30] However, for a cluster involving five (Figure 6) and six (Figure 8) water molecules, hydrolysis of the initial reactant structures each containing strongly *ionized* N_2O_5 leads to reaction products containing both the *ionic* ($H_3O^+NO_3^-$) and *molecular* acids. Within these product structures the hydroxonium and nitrate ions are separated by double rings of water molecules in cage structures. Recent ab initio investigations have shown that analogous small water clusters can stabilize other ionized acids in this way.[66,67] Along the reaction pathways we have identified, the formation of two ion pairs is unlikely in the initial step, however the *molecular* acid may dissociate upon further solvation.

We turn now to consider the energetics of the hydrolysis reaction. Tabazadeh et al.[42] have estimated the barrier for hydrolysis to be 6.2 kcal mol^{-1} on PSC aerosols using a physical chemistry model. We report a difference in reactivity of N_2O_5 that depends on the structure of the adsorption site and the extent of ionization of N_2O_5. For the reaction catalyzed by three waters (Figure 3) the barrier is 13.3 kcal mol^{-1} (Table 4). However, increasing the number of solvating water molecules to four and five waters (Figures 4 and 5) leads to an *increase* in the barrier for hydrolysis to 19.6 and 15.8 kcal mol^{-1} respectively (Table 4). By consideration of the corresponding reactant structures (Figures 4a and 5a) the *decrease* in the N_1-O_4 distances going from the three-water system to the four- and five-water clusters, reflects a decrease in the ionicity of the N_2O_5 species and thus an *increase* in the hydrolysis barrier. For the clusters involving five (Figure 6) and six (Figure 8) water molecules hydrolysis barriers of 7.7 and 3.4 kcal mol^{-1} suggest that the reaction under stratospheric conditions, where additional waters may be present as part of the ice surface, will proceed effectively without a barrier. Thus we predict a facile hydrolysis reaction on PSC ice aerosol surfaces, where different adsorption sites are available for solvation.

Finally we comment on the structure of the water clusters used to model the PSC ice aerosol surface. Our reactant structures involving rings of water molecules (Figures 2−7) are related to the rings reported on the annealed ice surface studied by Buch et al.[63] In the larger structures containing five and six water molecules (Figures 6 and 7) these model systems each contain a single ring of water molecules with additional adsorbed molecules on top of the ring. In the five-water cluster (isomer 2, Figure 6) the surface adsorbed water is able to promote ionization of N_2O_5 and stabilize the developing ion pair. However, in the other five-water cluster (isomer 1, Figure 5) the extra water molecule is in the plane of the ring and is unable to affect ionization. Thus surface adsorbed waters may be important in solvating developing ion pairs. The structures containing four, five, and six water molecules (Figures 8 and 9) are all closely related to ice. The molecular surface structure of a low-temperature hexagonal ice crystal has been probed by Materer et al.[58] in which they found that the surface had full bilayer termination. Thus these models contain structural arrangements of water molecules *representative* of the hexagonal ice surface. Notably, the reactive sites we have considered each contain surface defects where adsorption is likely to be more favorable than on the full bilayer terminated surface. Evidently from both the ring and ice-like cluster models, solvation of the developing nitrate at O_6 and O_7 promotes ionization, thus leading to a lower barrier for hydrolysis. Bianco and Hynes[44] suggest these types of small water clusters are more closely related to supercooled water where the absence of lattice constraints mimic the increased flexibility of supercooled water compared to ice.

In summary our calculations have identified a difference in reactivity of N_2O_5 which depends on how the adsorption site modifies the structure of N_2O_5. The calculations suggest that the proposed intermediate[31] $H_2ONO_2^+$ is unlikely to be involved in the ice-catalyzed reaction although further increasing the size of our clusters may lead to increased ionization of N_2O_5. Our range of model clusters has accounted for a number of different adsorption sites likely to be found on the PSC ice aerosol. However our central finding of atmospheric importance,[1−17] is that N_2O_5 is readily hydrolyzed in neutral water clusters, of a relatively small critical size, that do not require larger aerosols or ion containing clusters.[8]

Acknowledgment. We thank EPSRC for support of this research and Dr. J. C. Whitehead for helpful discussion.

Supporting Information Available: Cartesian geometries, energies, and vibrational frequencies are available for all stationary structures (minima and TSs) discussed in the text. This material is available free of charge via the Internet at http://pubs.acs.org.

References and Notes

(1) Solomon, S.; Garcia, R. R.; Rowland, F. S.; Wuebbles, D. J. *Nature* **1986**, *321*, 755.

(2) Solomon, S. *Rev. Geophys.* **1988**, *26*, 131.

(3) Solomon, S. *Nature* **1990**, *347*, 347.

(4) Tolbert, M. A. *Science* **1994**, *264*, 527.

(5) McElroy, M. B.; Salawitch, R. J.; Wofsy, S. C. *Geophys. Res. Lett.* **1986**, *13*, 1296.

(6) Turco, R. P.; Toon, O. B.; Hamill, P. J. *Geophys. Res.* **1989**, *94*, 16493.

(7) Cicerone, R. J. *Science* **1987**, *237*, 35.

(8) Crutzen, P. J.; Arnold, F. *Nature* **1986**, *324*, 651.

(9) Molina, M. J.; Rowland, F. S. *Nature* **1974**, *249*, 810.

(10) Molina, M. J.; Tso, T.-L.; Molina, L. T.; Wang, F. C.-Y. *Science* **1987**, *238*, 1253.

(11) Henderson, G. S.; Evans, W. F. J.; McConnell, J. C. *J. Geophys. Res.* **1990**, *95*, 1899.

(12) Wennberg, P. O.; Cohen, R. C.; Stimpfle, R. M.; Koplow, J. P.; Anderson, J. G.; Salawitch, R. J.; Fahey, D. W.; Woodbridge, E. L.; Keim, E. R.; Gao, R. S.; Webster, C. R.; May, R. D.; Toohey, D. W.; Avallone, L. M.; Proffitt, M. H.; Loewenstein, M.; Podolske, J. R.; Chan, K. R.; Wofsy, S. C. *Science* **1994**, *266*, 398.

(13) Russell, A. G.; McRae, G. J.; Cass, G. R. *Atmos. Environ.* **1985**, *19*, 893.

(14) Rodriguez, J. M.; Ko, M. K. W., Sze, N. D. *Nature* **1991**, *352*, 134.

(15) Webster, C. R.; May, R. D.; Toumi, R.; Pyle, J. A. *J. Geophys. Res.* **1990**, *95*, 13 851.

(16) Dentener, F. J.; Crutzen, P. J. *J. Geophys. Res.* **1993**, *98*, 7149.

(17) Kumer, J. B.; Kawa, S. R.; Roche, A. E.; Mergenthaler, J. L.; Smith, S. E.; Taylor, F. W.; Connell, P. S.; Douglass, A. R. *J. Geophys. Res.* **1997**, *102*, 3575.

(18) Mentel, T. F.; Bleilebens, D.; Wahner, A. *Atmos. Environ.* **1996**, *30*, 4007.

(19) Hanson, D. R.; Ravishankara, A. R. *J. Geophys. Res.* **1991**, *96*, 5081.

(20) Quinlan, M. A.; Reihs, C. M.; Golden, D. M.; Tolbert, M. A. *J. Phys. Chem.* **1990**, *94*, 3255.

(21) Leu, M.-T. *Geophys. Res. Lett.* **1988**, *15*, 851.

(22) Hanson, D. R.; Ravishankara, A. R. *J. Geophys. Res.* **1991**, *96*, 17 307.

(23) Hanson, D. R.; Lovejoy, E. R. *Geophys. Res. Lett.* **1994**, *21*, 2401.

(24) Hanson, D. R. *Geophys. Res. Lett.* **1997**, *24*, 1087.

(25) Wincel, H.; Mereand, E.; Castleman, A. W., Jr. *J. Phys. Chem.* **1994**, *98*, 8606.

(26) Wincel, H.; Mereand, E.; Castleman, A. W., Jr. *J. Chem. Phys.* **1995**, *102*, 9228.

(27) Morris, E. D., Jr.; Niki, H. *J. Phys. Chem.* **1973**, *77*, 1929.

(28) Tuazon, E. C.; Atkinson, R.; Plum, C. N.; Winer, A. M.; Pitts, J. N., Jr. *J. Geophys. Res. Lett.* **1983**, *10*, 953.

(29) Hjorth, J.; Ottobrini, G.; Cappellani, F.; Restelli, G. *J. Phys. Chem.* **1987**, *91*, 1565.

(30) Horn, A. B.; Koch, T.; Chesters, M. A.; McCoustra, M. R. S.; Sodeau, J. R. *J. Phys. Chem.* **1994**, *98*, 946.

(31) Koch, T. G.; Banham, S. F.; Sodeau, J. R.; Horn, A. B.; McCoustra, M. R. S.; Chesters, M. A. *J. Geophys. Res.* **1997**, *102*, 1513.

(32) Koch, T. G.; Horn, A. B.; Chesters, M. A.; McCoustra, M. R. S.; Sodeau, J. R. *J. Phys. Chem.* **1995**, *99*, 8362.

(33) Cantrell, C. A.; Shetter, R. E.; Calvert, J. G.; Tyndall, G. S.; Orlando, J. J. *J. Phys. Chem.* **1993**, *97*, 9141.

(34) Angel, L.; Stace, A. J. *J. Chem. Soc., Faraday Trans.* **1997**, *93*, 2769.

(35) Parthiban, S.; Raghunandan, B. N.; Sumathi, R. *J. Mol. Struct. (THEOCHEM)* **1996**, *367*, 111.

(36) McClelland, B. W.; Hedberg, L.; Hedberg, K.; Hagen, K. *J. Am. Chem. Soc.* **1983**, *105*, 3789.

(37) Stirling, A.; Pápai, I.; Mink, J.; Salahub, D. R. *J. Chem. Phys.* **1994**, *100*, 2910.

(38) Bencivenni, L.; Sanna, N.; Schriver-Mazzouli, L.; Schriver, A. *J. Chem. Phys.* **1996**, *104*, 7836.

(39) Zhun, I.; Zhou, X.; Liu, R. *J. Chem. Phys.* **1996**, *105*, 11 366.

(40) Grabow, J.-U.; Andrews, A. M.; Fraser, G. T.; Irikura, K. K.; Suenram, R. D.; Lovas, F. J.; Lafferty, W. J.; Domenech, J. L. *J. Chem. Phys.* **1996**, *105*, 7249.

(41) Hanway, D.; Tao, F.-M. *Chem. Phys. Lett.* **1998**, *285*, 459.

(42) Tabazadeh. A.; Turco, R. P. *J. Geophys. Res.* **1993**, *98*, 12 727.

(43) Snyder, J. A.; Hanway, D.; Mendez, J.; Jamka, A. J.; Tao, F.-M. *J. Phys. Chem.* **1999**, *103*, 9355.

(44) Bianco, R.; Hynes, J. T. *Int. J. Quantum Chem.* **1999**, *75*, 683.

(45) McNamara, J. P.; Tresadern, G.; Hillier, I. H. *J. Phys. Chem. A* **2000**, in press.

(46) Bianco, R.; Hynes, J. T. *J. Phys. Chem. A* **1999**, *103*, 3797.

(47) Haas, B.-M.; Crellin, K. C.; Kuwata, K. T.; Okumura, M. *J. Phys. Chem.* **1994**, *98*, 6740.

(48) Mebel, A. M.; Morokuma, K. *J. Phys. Chem. A* **1996**, *100*, 2985.

(49) McNamara, J. P.; Tresadern, G.; Hillier, I. H. *Chem. Phys. Lett.* **1999**, *310*, 265.

(50) McNamara, J. P.; Hillier, I. H. *J. Phys. Chem. A* **1999**, *103*, 7310.

(51) Bianco, R.; Hynes, J. T. *J. Phys. Chem. A* **1998**, *102*, 309.

(52) Xu, S. C.; Zhao, X. S. *J. Phys. Chem. A* **1999**, *103*, 2100.

(53) Akhmatskaya, E. V.; Apps, C. J.; Hillier, I. H.; Masters, A. J.; Palmer, I. J.; Watt, N. E.; Vincent, M. A.; Whitehead, J. C. *J. Chem. Soc., Faraday Trans.* **1997**, *93*, 2775.

(54) La Manna, G. *J. Mol. Struct. (THEOCHEM)* **1994**, *309*, 31.

(55) Lee, C.; Vanderbilt, D.; Laasonen, K.; Car, R.; Parrinello, M. *Phys. Rev. B* **1993**, *47*, 4863.

(56) Bernal, J. D.; Fowler, R. H., *J. Chem. Phys.* **1933**, *8*, 515.

(57) Davidson, E. R.; Morokuma, K. *J. Chem. Phys.* **1984**, *81*, 3741.

(58) Materer, N.; Starke, U.; Barbieri, A.; Van Hove, M. A.; Somorjai, G. A.; Kroes, G.-J.; Minot, C. *J. Phys. Chem.* **1995**, *99*, 6267.

(59) Silva, S. C.; Devlin, J. P. *J. Phys. Chem.* **1994**, *98*, 10847.

(60) Devlin, J. P.; Buch, V. *J. Phys. Chem.* **1995**, *99*, 16534.

(61) Devlin, J. P.; Buch, V. *J. Phys. Chem. B* **1997**, *101*, 6095.

(62) Rowland, B.; Kadagathur, N. S.; Devlin, J. P.; Buch, V.; Feldman, T.; Wojcik, M. J. *J. Phys. Chem.* **1995**, *99*, 8328.

(63) Buch, V.; Delzeit, L.; Blackledge, C.; Devlin, J. P. *J. Phys. Chem.* **1996**, *100*, 3732.

(64) Geiger, F. M.; Hicks, J. M.; de Dios, A. C. *J. Phys. Chem. A* **1998**, *102*, 1514.

(65) Robinson Brown, A.; Doren, D. J. *J. Phys. Chem. B* **1997**, *101*, 6308.

(66) Vincent, M. A.; Palmer, I. J.; Hillier, I. H.; Akhmatskaya, E. V. *J. Am. Chem. Soc.* **1998**, *120*, 3431.

(67) Smith, A.; Vincent, M. A.; Hillier, I. H. *J. Phys. Chem. A* **1999**, *103*, 1132.

(68) George, S. M.; Livingston, F. E. *Surf. Rev. Lett.* **1994**, *4*, 771.

(69) Frisch, M. J.; Trucks, G. W.; Schlegel, H. B.; Gill, P. M. W.; Johnson, B. G.; Robb, M. A.; Cheeseman, J. R.; Keith, T. A.; Petersson, G. A.; Montgomery, J. A.; Raghavachari, K.; Al-Laham, M. A.; Zakrzewski, V. G.; Ortiz, J. V Foresman, J. B.; Cioslowski, J.; Stefanov, B. B.; Nanayakkara, A.; Challacombe, M.; Peng, C. Y.; Ayala, P. Y.; Chen, W.; Wong, M. W.; Andres, J. L.; Replogle, E. S.; Gomperts, R.; Martin, R. L.; Fox, D. J.; Binkley, J. S.; Defrees, D. J.; Baker, J.; Stewart, J. P.; Head-Gordon, M.; Gonzalez G.; Pople, J. A. *GAUSSIAN94*, revision E.1; Gaussian, Inc.; Pittsburgh, PA, 1995.

(70) Frisch, M. J.; Trucks, G. W.; Schlegel, H. B.; Scuseria, G. E.; Robb, M. A.; Cheeseman, J. R.; Zakrzewski, V. G.; Montgomery, J. A.; Stratmann, R. E.; Burant, J. C.; Dapprich, S.; Millam, J. M.; Daniels, A. D.; Kudin, K. N.; Strain, M. C.; Farkas, O.; Tomasi, J.; Barone, V.; Cossi, M.; Cammi, R.; Mennucci, K.; Pomelli, C.; Adamo, C.; Clifford, S.; Ochterski, J.; Petersson, G. A.; Ayala, P. Y.; Cui, Q.; Morokuma, K.; Malick, D. K.; Rabuck, A. D.; Raghavachari, K.; Foresman, J. B.; Cioslowski, J.; Ortiz, J. V.; Sefanov, B. B.; Liu, G.; Liashenko, A.; Piskorz, P.; Komaromi, I.; Gomperts, R.; Martin, R. L.; Fox, D. J.; Keith, T.; Al-Laham, M. A.; Peng, C. Y.; Nanayakkara, A.; Gonzalez, C.; Challacombe, M.; Gill, P. M. W.; Johnson, B. G.; Chen, W.; Wong, M. W.; Andres, J. L.; Head-Gordon, M.; Replogle E. S.; Pople, J. A. *GAUSSIAN98*, revision A.1; Gaussian, Inc.; Pittsburgh, PA, 1998.

(71) Lee, C.; Yang, W.; Parr, R. G. *Phys. Rev. B* **1988**, *37*, 785.

(72) Miehlich, B.; Savin, A.; Stoll, H.; Preuss, H. *Chem. Phys. Lett.* **1989**, *157*, 200.

(73) Becke, A. D. *J. Chem. Phys.* **1993**, *98*, 5648.

(74) Møller, C.; Plesset, M. S. *Phys. Rev.* **1934**, *46*, 618.

(75) Banham, S. F.; Horn, A. B.; Koch, T. G.; Sodeau, J. R. *Faraday Discuss.* **1995**, *100*, 321.

(76) Sodeau, J. R.; Horn, A. B.; Banham, S. F.; Koch, T. G. *J. Phys. Chem.* **1995**, *99*, 6258.

(77) Horn, A. B.; Sodeau, J. R.; Roddis, T. B.; Williams, N. A. *J. Chem. Soc., Faraday Trans.* **1998**, *94*, 1721.

(78) Horn, A. B.; Sodeau, J. R.; Roddis, T. B.; Williams, N. A. *J. Phys. Chem. A* **1998**, *102*, 6107.